CLIC Detector Calibration with Physics Data

OUTLINE

- Introduction
- Expected Luminosities; nominal and at start
- Fast simulation software and parameters
- Calibration at 350 GeV; cross sections, muon rates for alignment, δP/P, P scale, δE/E; E scale
- Calibration at 1.4 TeV; stress the issues
- Calibration at 91.2 GeV; focus on what is unique
- Summary and outlook

Introduction

CLIC will run according to a staging scenario at $\sqrt{s}$=350 GeV, 1.4 Tev and 3 TeV.

At each energy detector alignment and calibration is essential to reach good physics performance.

The main issues to address are:

- Muon and Tracking systems alignment
- Charged particle momentum resolution and scale
- Calorimeter calibration, ECAL, HCAL, FCAL
- Di-jet energy resolution and scale
- Heavy flavor tagging efficiency
- Missing Et performance

Introduction

Accurate detector alignment can only be done after detector assembly. After alignment the calibration steps are:

- Measurement of the charged particle momentum resolution; Data/Monte Carlo comparison; Determination of the momentum scale using the invariant mass of well known particles, e.g MZ and MK^0s
- ECAL and HCAL calibration using electrons and isolated charged hadrons and comparing the energy deposition in the calorimeters with the track momentum.
- Measurement of di-jet energy resolution using di-jets origination from Z or W bosons; di-jet energy scale
- Heavy flavour tagging efficiency measurement using Zs.

Luminosities

√s Gev	Luminosity $cm^{-2}s^{1}$	Luminosity Per day, pb^{-1}	Luminosity Per day pb^{-1} in year-1	Luminosity Per day pb^{-1} in year-2
350	$1.5\ 10^{34}$	1300	65	325
1400	$3.7\ 10^{34}$	3200	160	800
3000	$5.9\ 10^{34}$	5100	255	1275
91.2	$2.3\ 10^{32}$	20	1	5

Expected nominal luminosities at CLIC.
At each centre-of-mass energy for the first three years the luminosity is reduced. The reduction factor is 5%, 25%, 50% for year-1, y-2, y-3.
Must be taken into account for the calibration strategy.

Fast Simulation

The WHIZARD program is used to compute the cross sections and generate the events of the various processes considered for the detector calibration.
The luminosity spectrum is generated using GUINEAPIG it is interfaced to WHIZARD using Circe2; effects of initial state radiation (ISR) are also included in WHIZARD.
PYTHIA program is used for quark fragmentation and hadronisation and lepton final state radiation (FSR).

Fast Simulation

To take into account the detector resolution, the momentum and energy of the particles are smeared using different Gaussian resolution parameters according to the particle type.

- Charged particles

  $\sigma(P)/P = a.P \oplus b/\sqrt{\sin\theta} \oplus c.\cos\theta/\sin\theta$; with

  $a = 2.\ 10^{-5}$; curvature measurement contribution

  $b = 2.\ 10^{-3}$; multiple scattering contribution

  $c = 2.\ 10^{-4}$; angular resolution contribution
- Photons: $\sigma(E)/E = 0.15/\sqrt{E}$
- Neutral hadrons: $\sigma(E)/E = 0.55/\sqrt{E}$

Fast Simulation

The main contributions to the jet energy resolution are:

- Tracking efficiency
- Momentum resolution
- Calorimeter energy resolution
- Leakage
- Particle confusion (e, γ fragments; h±, h0^{o} fragments)
- Jet confusion

These contributions change with the energy.

Several of them can't be approximated in a fast simulation; e.g leakage, particle confusion.

This leads to an underestimation in the jet energy resolution

- Jet clustering done using Fastjet.

Cross Sections and Event Rates at $\sqrt{s}$=350 GeV

Calibration Process Alignment, $\delta P/P$, MS	σ[fb] $E\mu$>5 GeV; $10<\theta\mu<170°$	Lumi factor	Events/fb^{-1}
$e^+ e^- \rightarrow \mu^+ \mu^- (\gamma)$	2.0×10^3	1	2.0×10^3
$e^+ e^- \rightarrow$ e νe μ νμ (x2)	2×10^5	1	2×10^5
$e^+ e^- \rightarrow e^+ e^- \mu^+ \mu^-$	3×10^4	1	3×10^4
$e^- \gamma \rightarrow e \mu^+ \mu^-$ (x2)	2.8×10^5	0.45	1.3×10^5
$\gamma \gamma \rightarrow \mu^+ \mu^-$	6.4×10^5	0.23	1.5×10^5
All			4.7×10^5

Calibration Process $\delta Ej/Ej$, JES	σ[fb] Eq>10 GeV; $10<\theta q<170°$	Lumi factor	Events/fb^{-1}
$e^+ e^- \rightarrow q \bar{q} (\gamma)$	1.7×10^4	1	1.7×10^4
$e^+ e^- \rightarrow$ e νe $q \bar{q}$ (x2)	1.2×10^3	1	1.2×10^3
$e^+ e^- \rightarrow e^+ e^- q \bar{q}$	1.8×10^3	1	1.8×10^3
$e^- \gamma \rightarrow \nu q \bar{q}$ (x2)	1.1×10^3	0.45	5×10^2
$e^- \gamma \rightarrow e^- q \bar{q}$ (x2)	8×10^4	0.45	3.6×10^4

Alignment at √s=350 GeV
All $\mu^+\mu^-$ events; $\int L=1fb^{-1}$

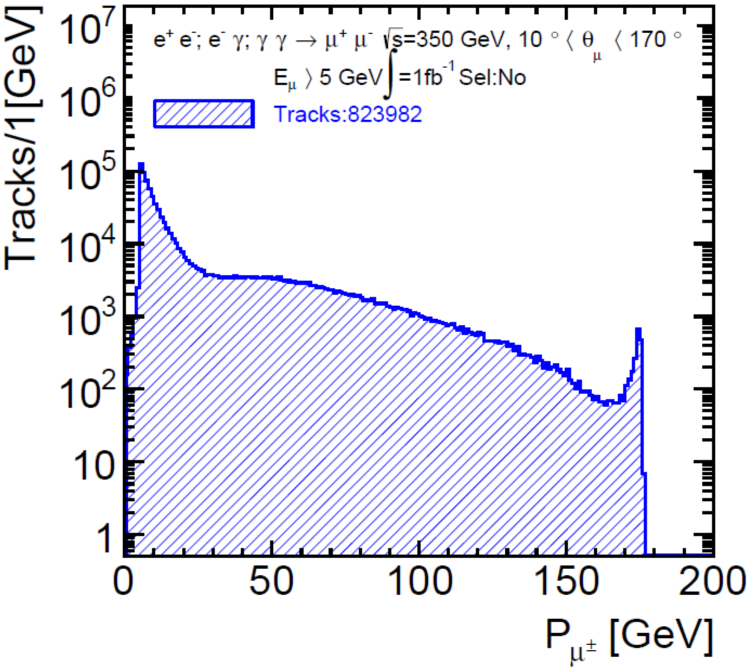

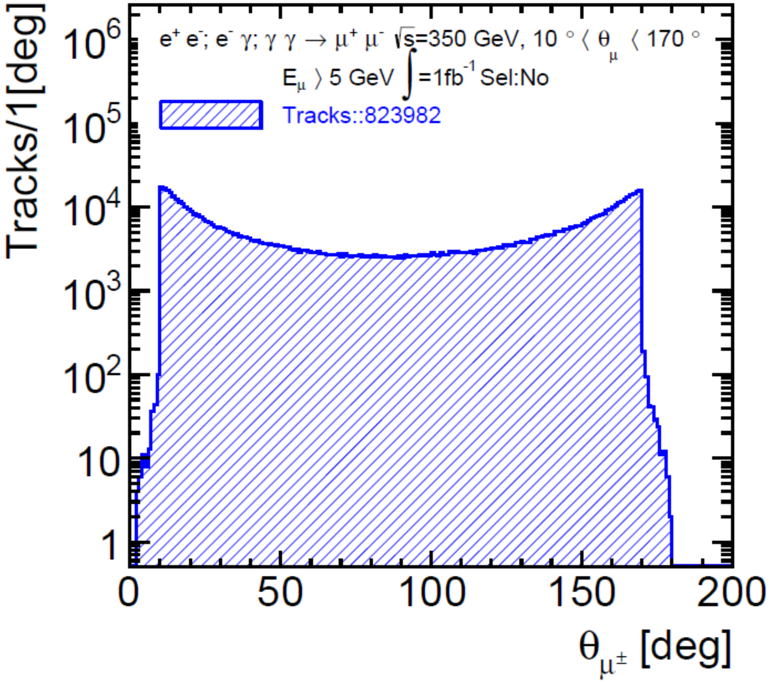

Left: dN/dPμ for $e^+ e^-$, $e^- \gamma$ and $\gamma \gamma \to \mu^+\mu^-$ x processes.
~ 800000 tracks ; Pμ range: 5-100 GeV
Right: dN/dθμ ; more than $5x10^3$ tracks/bin 1°
Year-1, 1 fb^{-1} <-> 15 days of run; beyond first year high muon rate allows regular control of alignment parameters.

Momentum Resolution and Scale at $\sqrt{s}$=350 GeV; $\int L=1fb^{-1}$

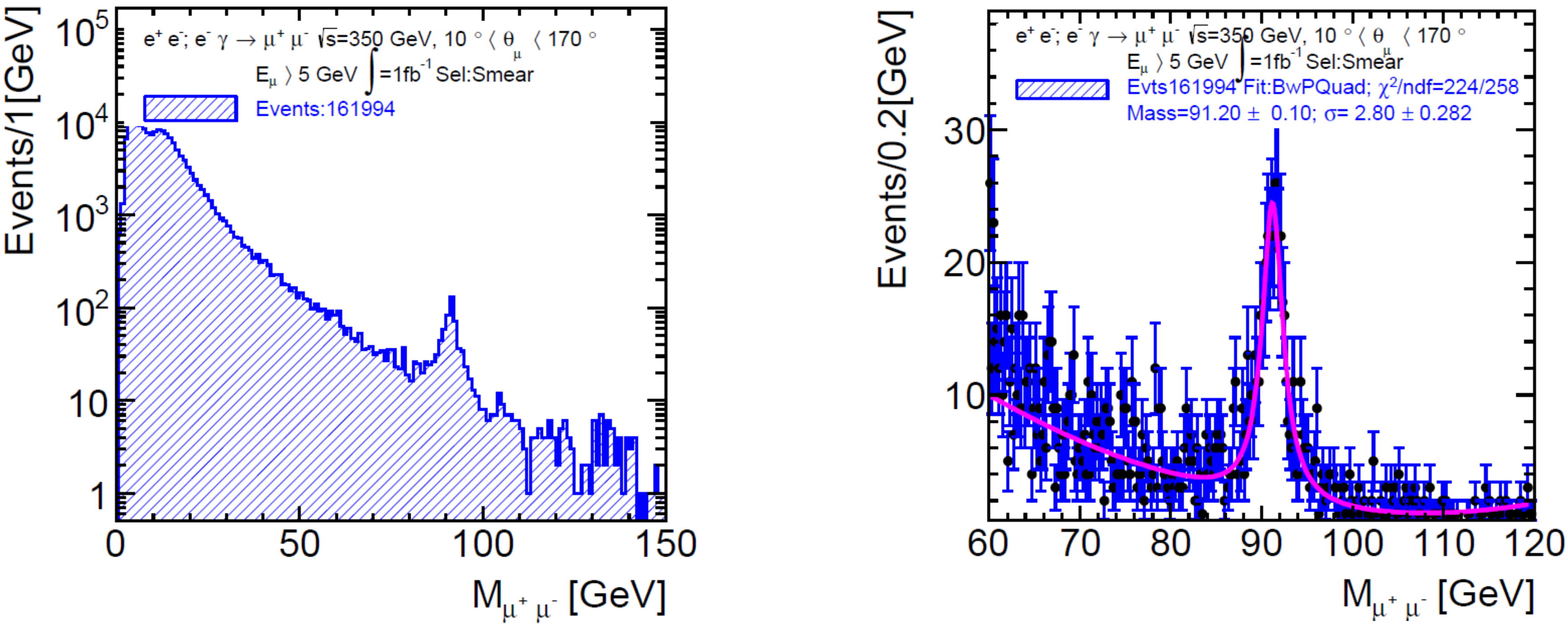

Left : $dN/dM(\mu^+\mu^-)$ with smearing of Pμ.

Right: Mass fit of the Z region; Fit BW + Background.

MZ=91.2 ± 0.1 GeV ; ΓZ=2.8±0.3; $\delta M/M=1x10^{-3}$

With more luminosity measure δM/M as a function of θ

Momentum Resolution and Scale at $\sqrt{s}$=350 GeV; ; $\int L=1fb^{-1}$

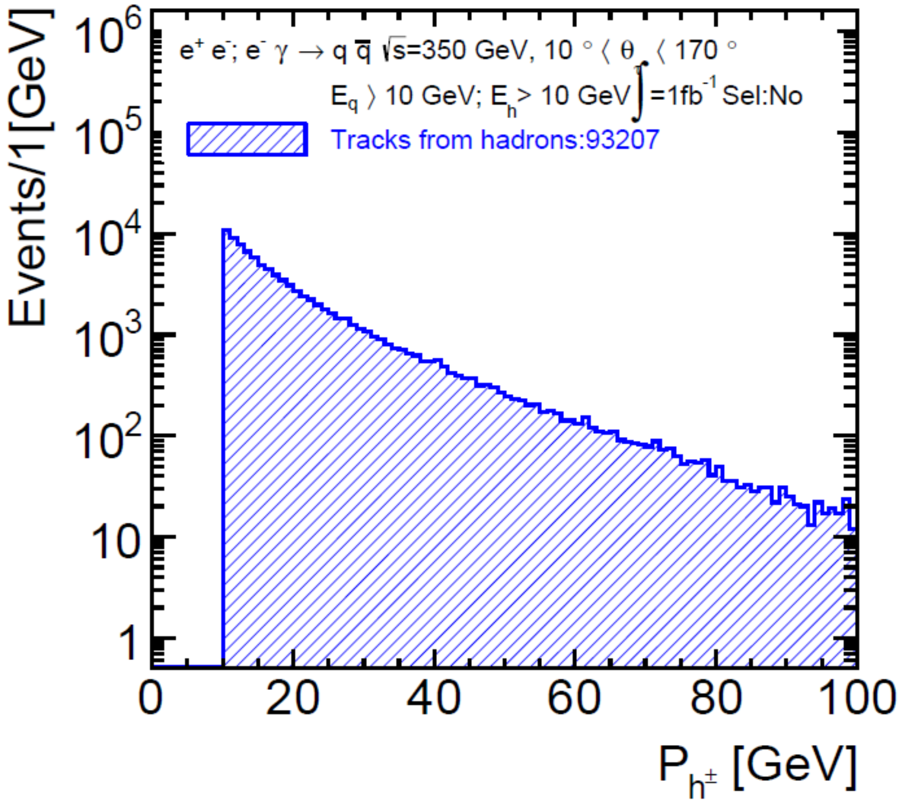

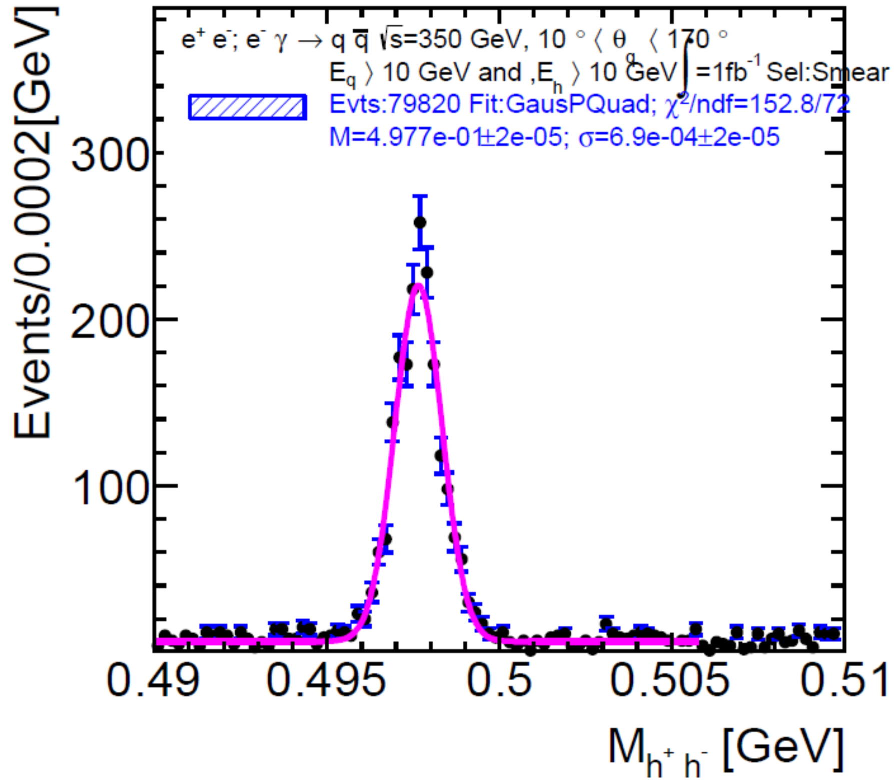

$e^+ e^- \rightarrow q\, \bar{q} \rightarrow K^0 s\ X \rightarrow \pi^+ \pi^- X$

Left : dN/dPh±;

Right: dN/dM ($\pi^+ \pi^-$) ; Mass Fit of K^0s region Gaus+Background

$MK^0s=0.4977 \pm 2x10^{-5}$; $\delta M/M=4x10^{-5}$

Di-jet Mass Resolution at √s=350 GeV ; ∫L=1fb^{-1}

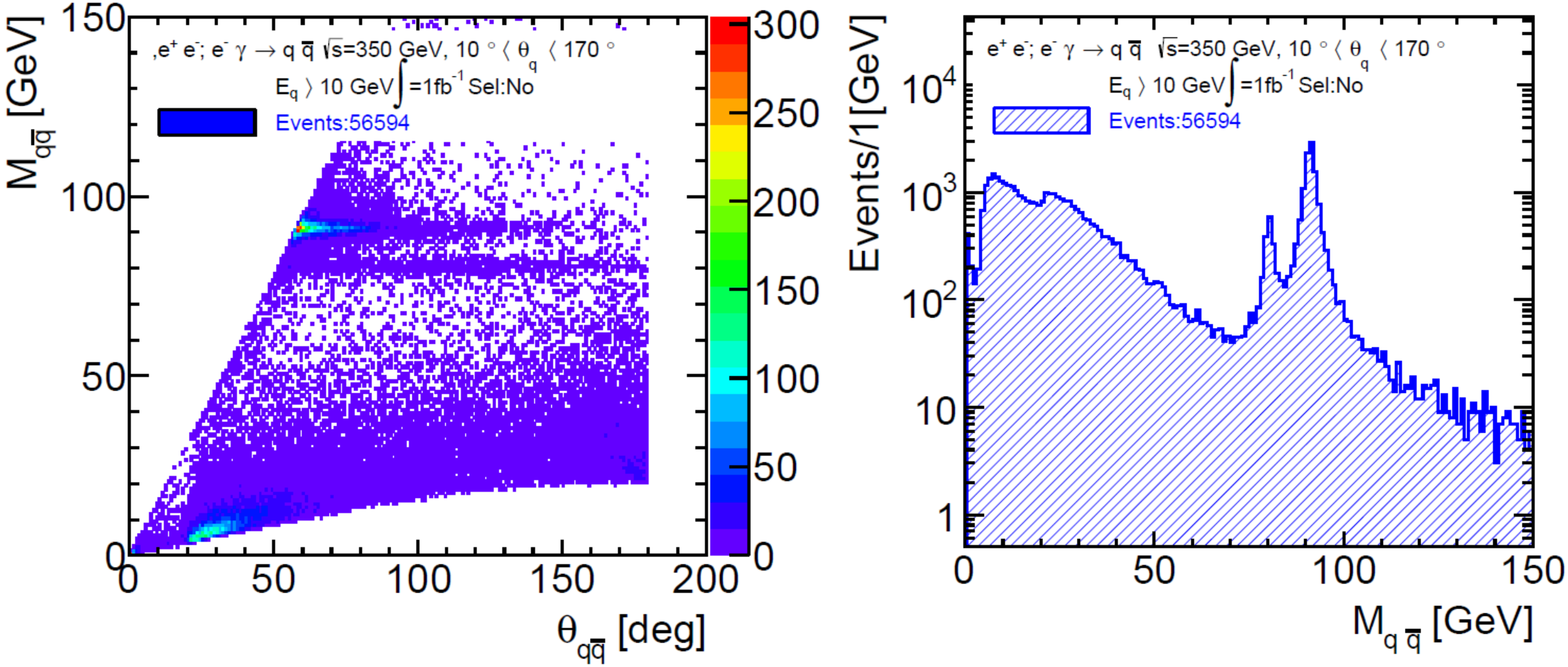

Left : Mqq̄ vs θqq̄; for $e^+ e^-$ and $e^- \gamma$ -> q q̄ x processes slide 8.

Z events ~ 60 °; W events θ ranges from 50 to 170°

Right: dN/dMqq̄; Largest contribution from Z→qq̄

Di-jet Mass Resolution at √s=350 GeV ; ∫L=1fb⁻¹

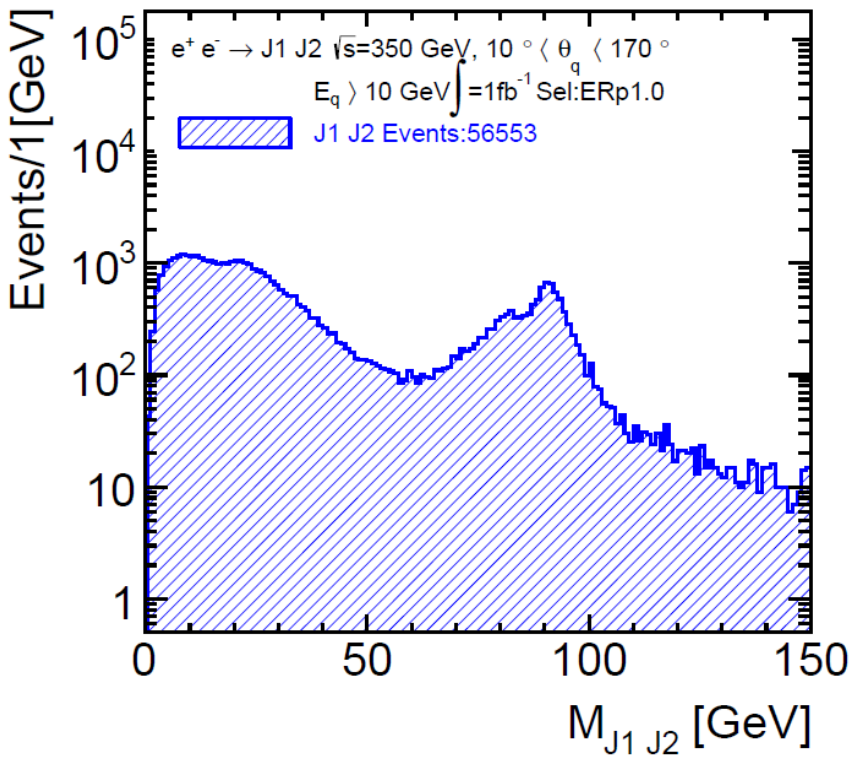

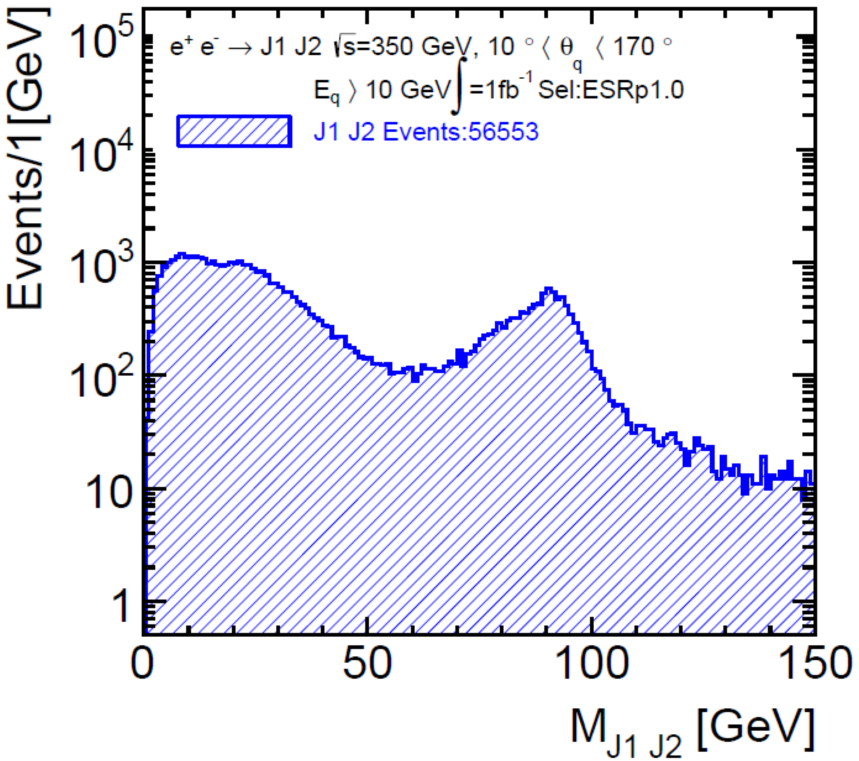

Left : dN/dMjj without P/E smearing; jet clustering; exclusive-kt, R=1
Right: dN/dMjj after P/E smearing an clustering
The W, Z separation is worse; the jet confusion has the strongest contribution to the di-jet mass resolution;

Di-jet Mass Resolution at $\sqrt{s}$=350 GeV ; $\int L=1fb^{-1}$

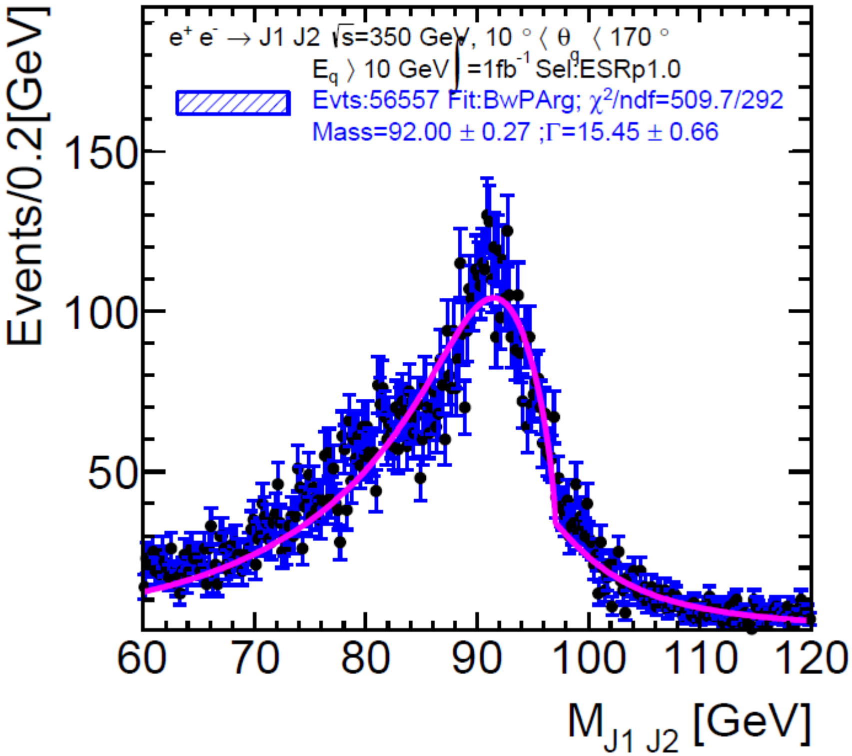

Zoom in Z, W region; W not visible; no W, Z separation.

MZ=92.0 ± 0.3 GeV; ΓZ=15.4 GeV

The resolution doesn't allow an accurate determination of the di-jet energy scale.

This data sample requires Monte Carlo corrections for heavy flavour tagging efficiency measurement.

After the second year

$e^+ e^- \rightarrow$ Z Z event rate significant

Use l l q q̄ events for flavor tagging efficiency measurement.

Cross Sections at √s=1400 GeV

Calibration Process Alignment, δP/P, MS	σ[fb] Eμ>5 GeV; 10<θμ<170°	Lumi factor	Events/fb^{-1}
$e^+ e^- \rightarrow \mu^+ \mu^- (\gamma)$	$2.0x10^2$ * MS $2.0x10^3$	1	$2.0x10^2$
$e^+ e^- \rightarrow$ e νe μ νμ (x2)	$6.5x10^5$	1	$6.5x10^5$
$e^+ e^- \rightarrow e^+ e^- \mu^+ \mu^-$	$3.8x10^4$	1	$3.8x10^4$
$e^- \gamma \rightarrow e \mu^+ \mu^-$ (x2)	$2.4x10^5$	0.75	$1.8x10^5$
$\gamma\ \gamma \rightarrow \mu^+ \mu^-$	$3.4x10^5$	0.64	$2.2x10^5$
All			$1.2x10^6$

Calibration Process δEj/Ej, JES	σ[fb] Eq>10 GeV; 10<θq<170°	Lumi factor	Events/fb^{-1}
$e^+ e^- \rightarrow q \bar{q} (\gamma)$	$1.2x10^3$ * ES $1.7x10^4$	1	$1.2x10^3$
$e^+ e^- \rightarrow$ e νe $q \bar{q}$ (x2)	$4.4x10^3$	1	$4.4x10^3$
$e^+ e^- \rightarrow e^+ e^- q \bar{q}$	$1.2x10^4$	1	$1.2x10^4$
$e^- \gamma \rightarrow \nu q \bar{q}$ (x2)	$2.5x10^4$	0.75	$1.9x10^4$
$e^- \gamma \rightarrow e^- q \bar{q}$ (x2)	$8.7x10^4$	0.75	$6.5x10^4$

Calibration at $\sqrt{s}$=1400 GeV $\int L=1fb^{-1}$

At 1.4 TeV; for alignment the main features are similar as at 350 GeV. All plots are included in the backup slides.

- Muon rates large; about 1.4 $x10^6$ tracks for $\int L=1fb^{-1}$ allow a regular control of the alignment parameters.
- $\sigma(e^+ e^- \rightarrow \mu^+ \mu^- (\gamma))=200\ fb^{-1}$; small; MZ can't be used during the first years for momentum scale calibration
- Use $e^+ e^- \rightarrow q \bar{q} \rightarrow K^0s\ X \rightarrow \pi^+ \pi^- X$

Jet energy resolution:

Di-jet Mass Resolution at √s=1400 GeV ; ∫L=1fb^{-1}

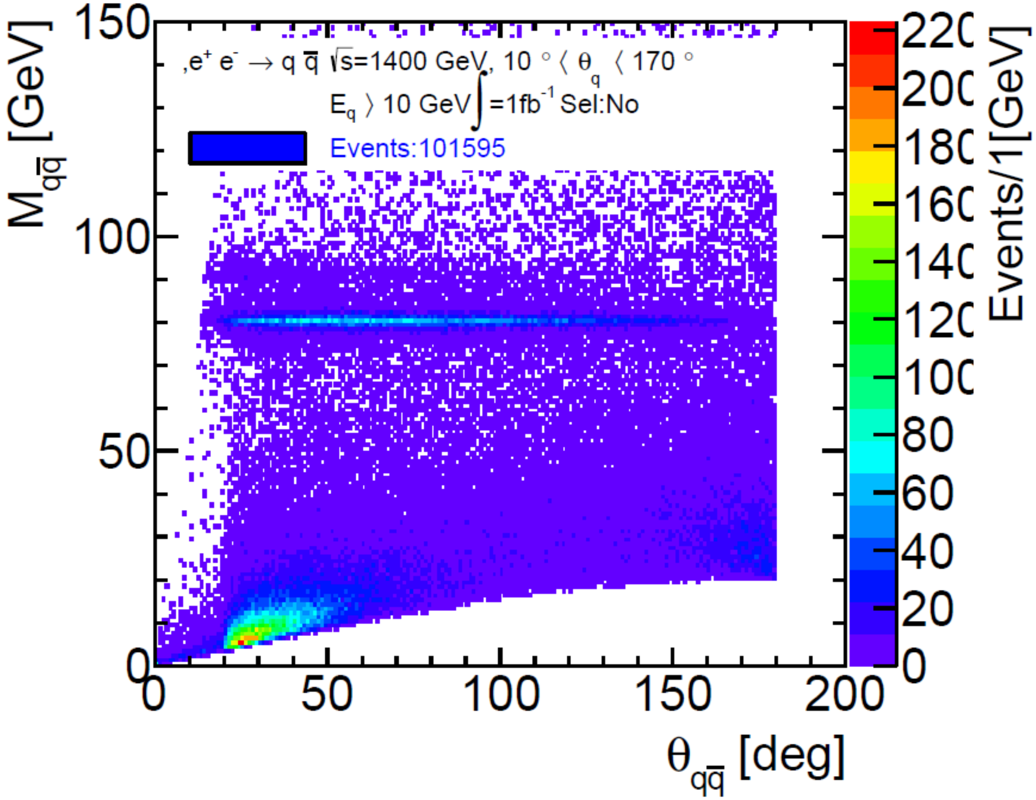

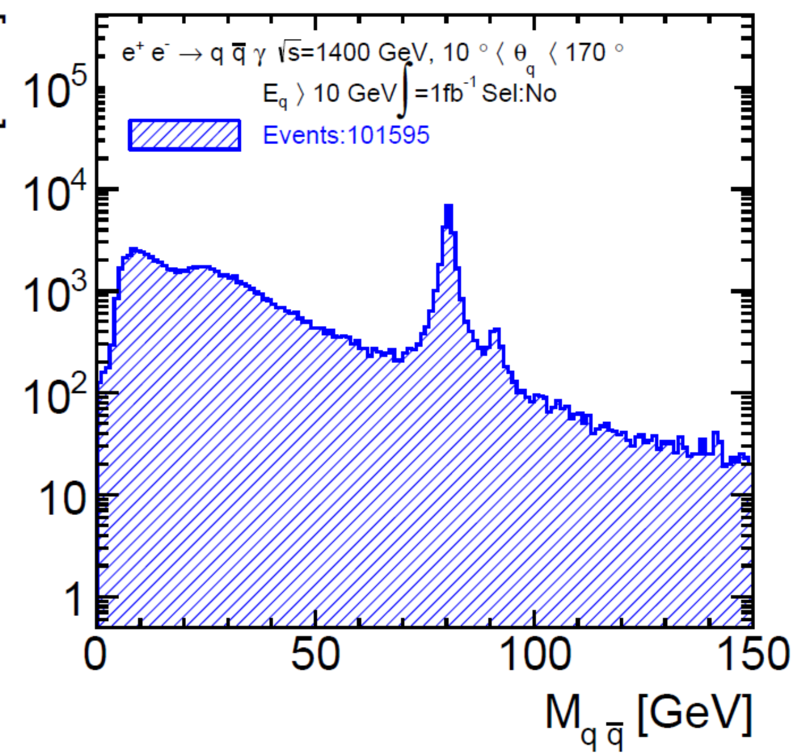

Left : Mq̄q vs θqq̄; W events θ ranges from 20 to 170°

Right: dN/dMqq̄; Large contribution from W→qq̄; Z → qq̄ small.

Di-jet Mass Resolution at $\sqrt{s}$=1400 GeV ; $\int L=1fb^{-1}$

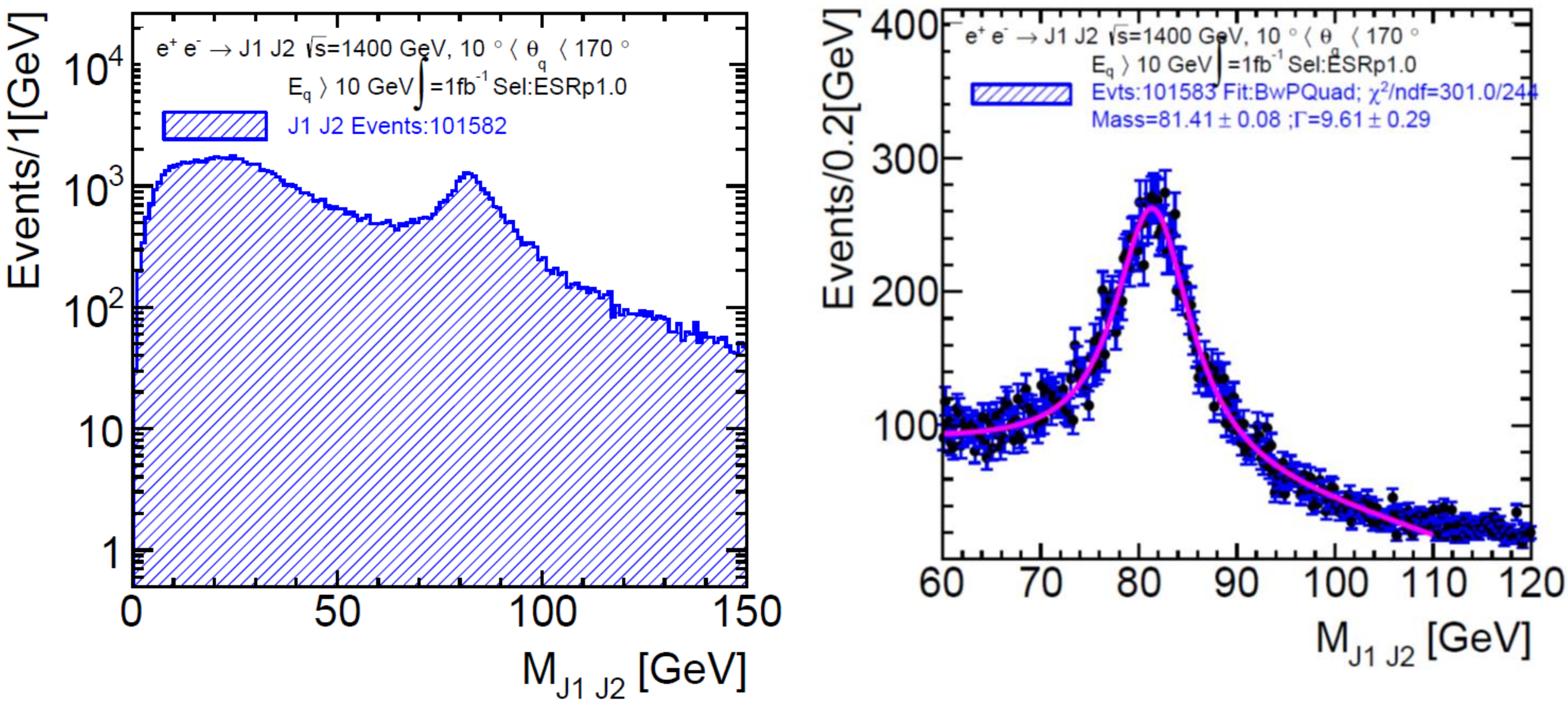

Left : dN/dMjj with P/E smearing; jet clustering; exclusive-kt, R=1
The Jet confusion leads to a poor di-jet mass resolution; allows data/MC comparison of the resolution; doesn't allow an accurate determination of the di-jet energy scale.

Cross Sections at √s=91.2 GeV

Calibration Process	σ[fb] Ef>10 GeV; 10<θ<170°	Events/pb^{-1}
$e^+ e^- \rightarrow \mu^+ \mu^- (\gamma)$	1.47×10^6	1.47×10^3
$e^+ e^- \rightarrow e^+ e^- (\gamma)$	5.70×10^6	5.70×10^3
$e^+ e^- \rightarrow \tau^+ \tau^- (\gamma)$	1.47×10^6	1.47×10^3
$e^+ e^- \rightarrow q \bar{q} (\gamma)$	29.6×10^6	29.6×10^3

Cross sections and number of events for $\int L=1\ pb^{-1}$.
The first year of CLIC running the luminosity is reduced and the Integrated luminosity per day is 1 pb^{-1}. The second year it should be 5 pb^{-1} providing significant event samples for calibration.
15000 back to back muons for momentum resolution /day
150000 back to back jets for energy resolution /day

Momentum Resolution and Scale at √s=91 GeV ; ∫L⁰=5pb⁻¹

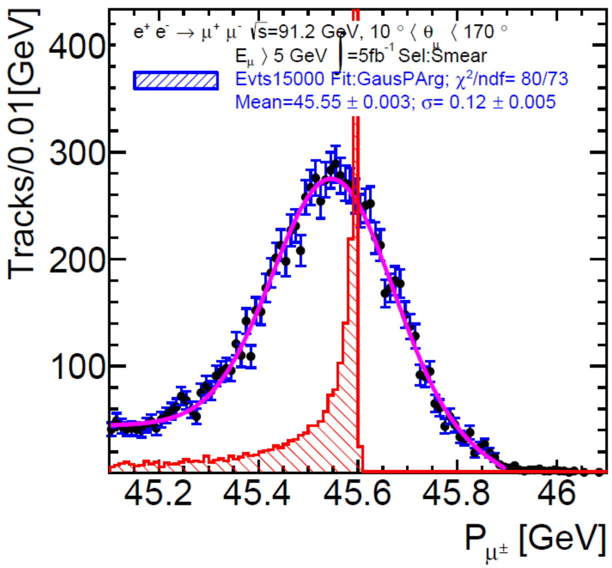

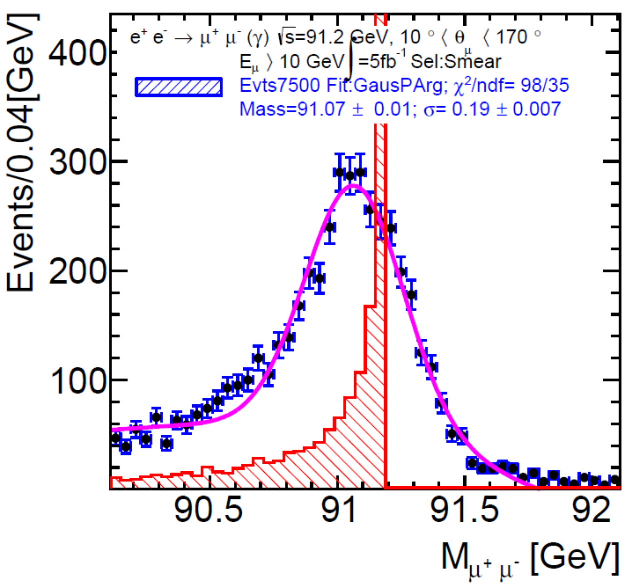

$e^+ e^- \rightarrow \mu^+\mu^- (\gamma)$

- dN/dP(μ);

With smearing (blue), without (red scaled)

Tail towards low P from events with Isr γ

<Pμ>=45.55 ± 0.003 GeV; σ=0.12 GeV

$\sigma(P\mu)/P\mu = 2.7\ 10^{-3}$.

Direct and accurate measurement of momentum resolution and scale.

- $dN/dM(\mu^+\mu^-)$;

With smearing (blue), without (red, scaled)

$<M\mu^+\mu^-> = 91.07 \pm 0.01$ GeV

σ=0.2±0.007; no Z width in production

Total Energy Resolution and Scale at √s=91 GeV; $\int L^0 = 5pb^{-1}$

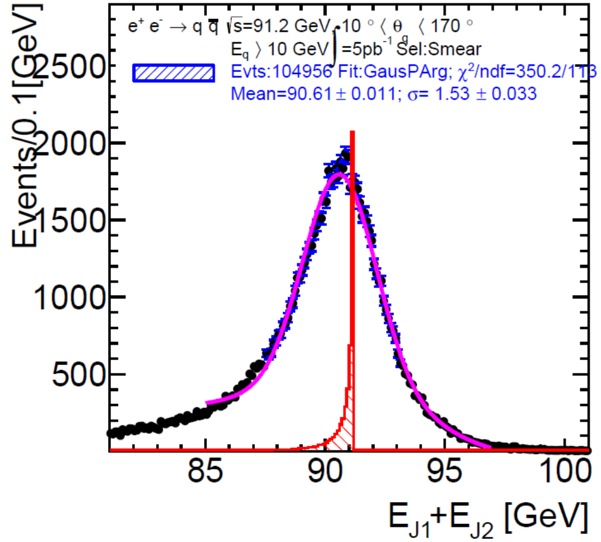

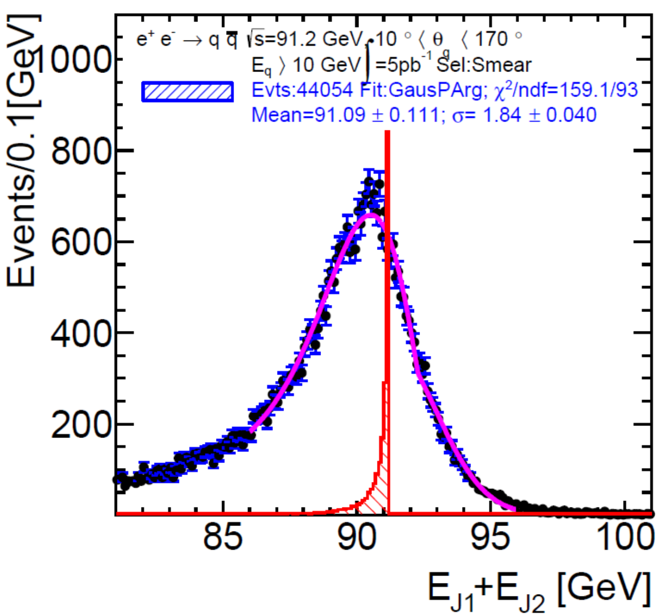

$e^+ e^- \rightarrow$ q q (γ) -> J1, J2

Particle smearing, no clustering,

- dN/dEtot in barrel

  <Etot>=90.61±0.011 GeV

Back to back jets; no jet confusion

σ(Etot)=1.53 GeV; σ(Etot)/Etot=1.7%

σ(Ej)/Ej=2.4% ; Full simulation 3.7%

Accurate measurement of the energy resolution and scale.

- dN/dEtot in endcap

<Etot>=91.09±0.11 GeV

σ(Etot)=1.84 GeV increase due to particles from jet escaping detection.

θ< 7° or θ> 173°

Summary

- At $\sqrt{s}$=350 GeV and 1.4 TeV the high muon rate allows detector alignment and regular control of alignment parameters.
- At $\sqrt{s}$=350 GeV, $Z \rightarrow \mu^+ \mu^-$ and $K^0 s \rightarrow \pi^+ \pi^-$ events allow a good control of the momentum resolution and a determination of the momentum scale
- At $\sqrt{s}$=350 GeV, di-jet events allow a control of the jet energy resolution, not an accurate determination of the JES. The poor Z, W separation leads to a Z sample with W contamination; (MC corrections heavy flavour tagging)
- $e^+ e^- \rightarrow$ ZZ event rate significant only after year-2

Summary

- At 1.4 TeV $\sigma(e^+ e^- \rightarrow \mu^+ \mu^- (\gamma))$=200 fb; during the first two years the momentum scale calibration can't be determined using the di-muon mass measurement.
  It relies on $K^0s \rightarrow \pi^+ \pi^-$events
- Most di-jet events originate from W's; it allows a control of the jet energy resolution, not an accurate determination of the JES.
- The di-jet rate originating from Zs is small; the poor Z, W separation doesn't allow Z identification
- Having flavour tagging efficiency is an issue.

Summary

At √s=91.2 GeV:

- $e^+ e^- \rightarrow \mu^+ \mu^- (\gamma)$ events provides a direct measurement of the momentum resolution at 45.6 GeV and an accurate determination of the momentum scale.
- The di-jet event sample allows a direct measurement of the di-jet energy resolution and an accurate determination of the di-jet energy scale.
  It allows also the flavour tagging efficiency measurement.

During the first stage of CLIC and after the first year, running at √=91.2 GeV provides unique calibration features and an excellent opportunity to optimize the detector performance

Outlook

Several contributions to the total energy resolution can't be approximated in a fast simulation.
To characterize more accurately the jet energy calibration performance at $\sqrt{}$=91.2 GeV would require full simulation and reconstruction.
At high energy the resolution is dominated by the jet confusion; full simulation would be necessary to estimate the degradation of the resolution coming from $\gamma\gamma \rightarrow$ hadron events.

Thanks

Alignment at √s=1400 GeV
All $\mu^+\mu^-$ events; $\int L=1fb^{-1}$

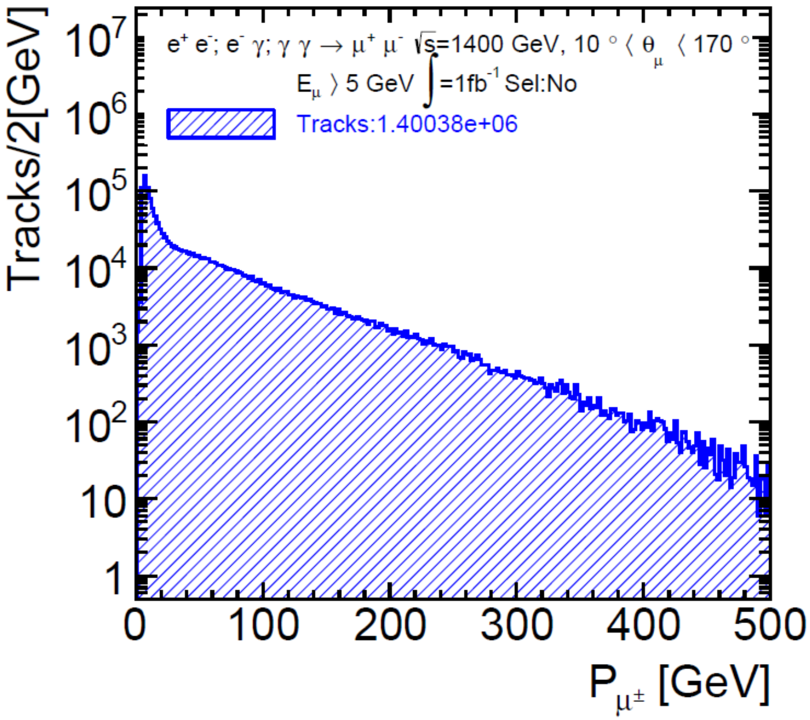

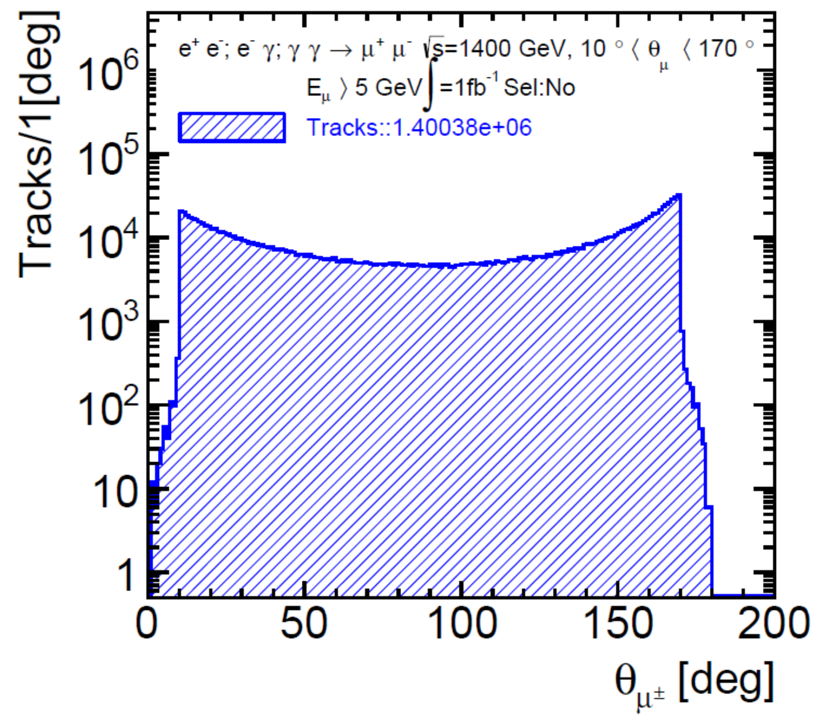

Left: $dN/dP\mu$ ~ 1.4 10^6 tracks ; Pμ range: 53100 GeV
Right: $dN/d\theta\mu$; ~10^4 tracks/bin 1°
Year-1, 1 fb^{-1} <-> 6 days of run; beyond first year high muon rate allows regular control of alignment parameters.

Momentum Resolution and Scale at √s=1400 GeV; ; ∫L=1fb^{-1}

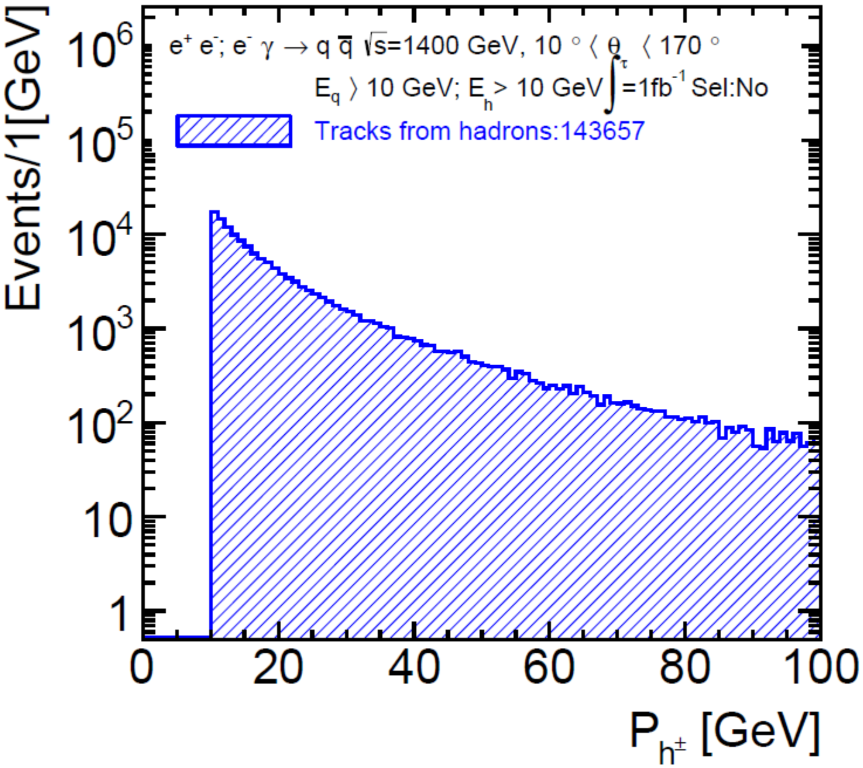

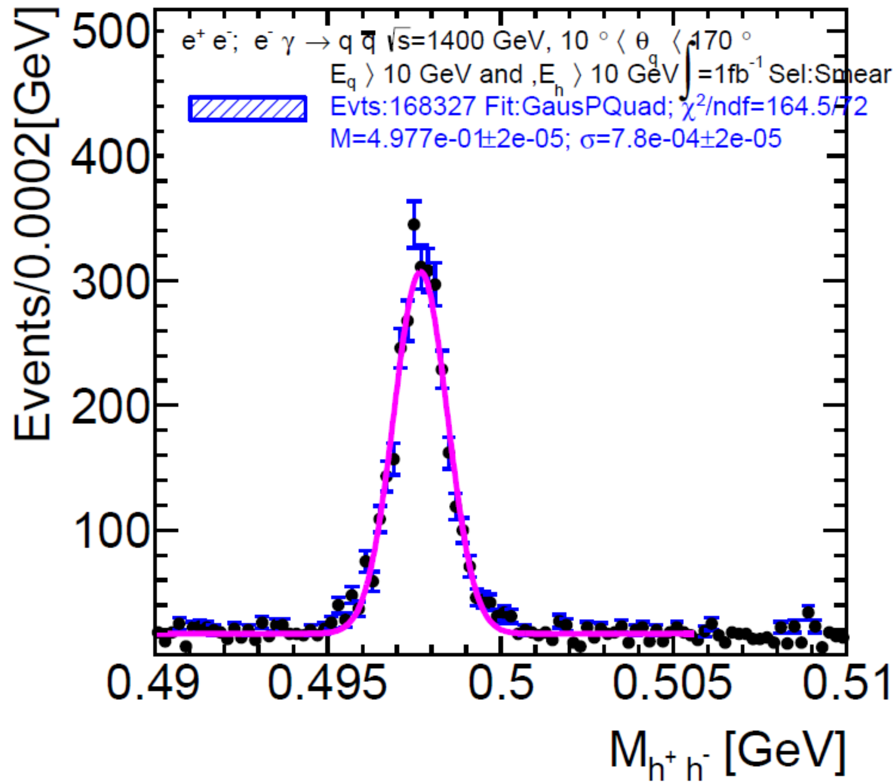

$e^+ e^- \rightarrow q\,\bar{q} \rightarrow K^0s\ X \rightarrow \pi^+ \pi^-\ X$

Left : dN/dPh;

Right: dN/dM ($\pi^+ \pi^-$) ; Mass Fit of K^0s region Gaus+Background

$MK^0s=0.4977 \pm 2\times10^{-5}$; $\delta M/M=4\times10^{-5}$

Di-jet Mass Resolution at $\sqrt{s}$=1400 GeV ; $\int L = 1 fb^{-1}$

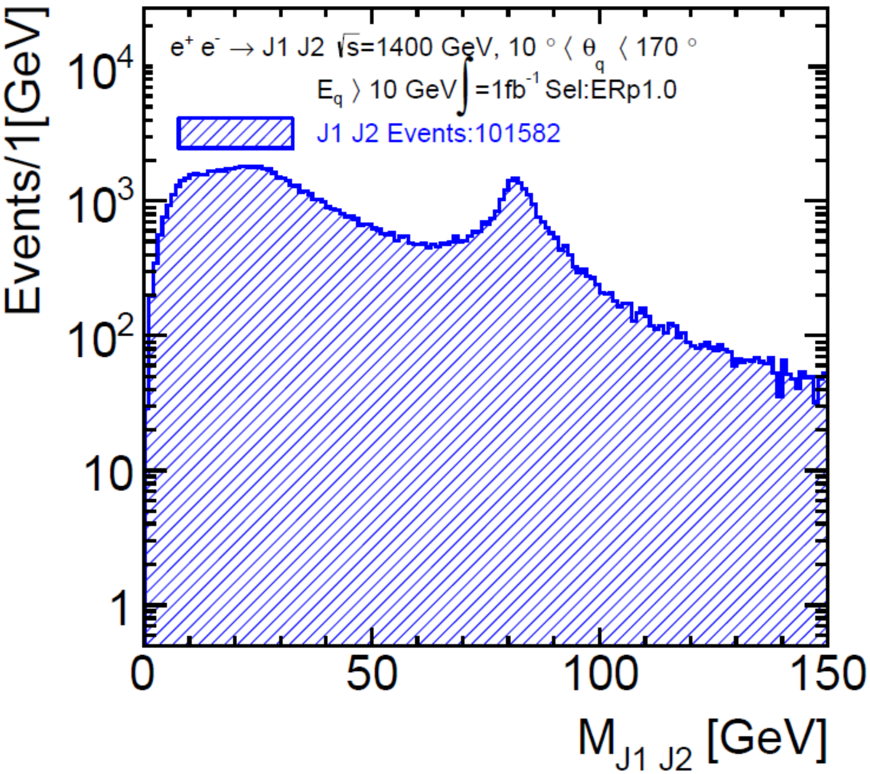

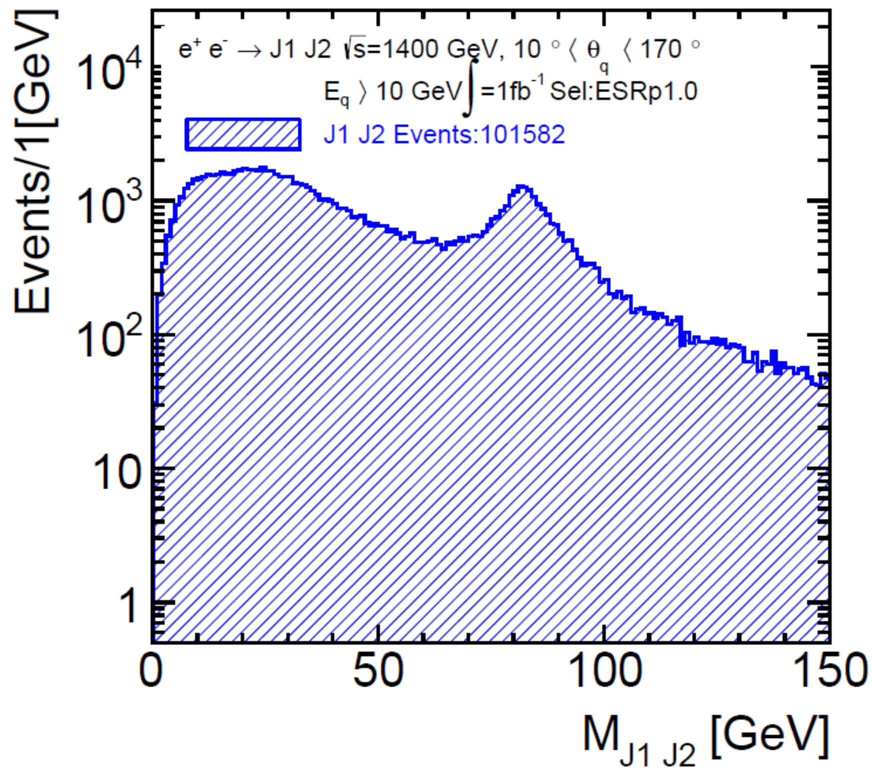

Left : dN/dMjj without P/E smearing; jet clustering; exclusive-kt, R=1

Right: dN/dMjj after P/E smearing an clustering

The Jet confusion has the strongest contribution to the di-jet mass resolution.

Di-jet Mass Resolution at √s=1400 GeV ; ∫L=1fb^{-1}

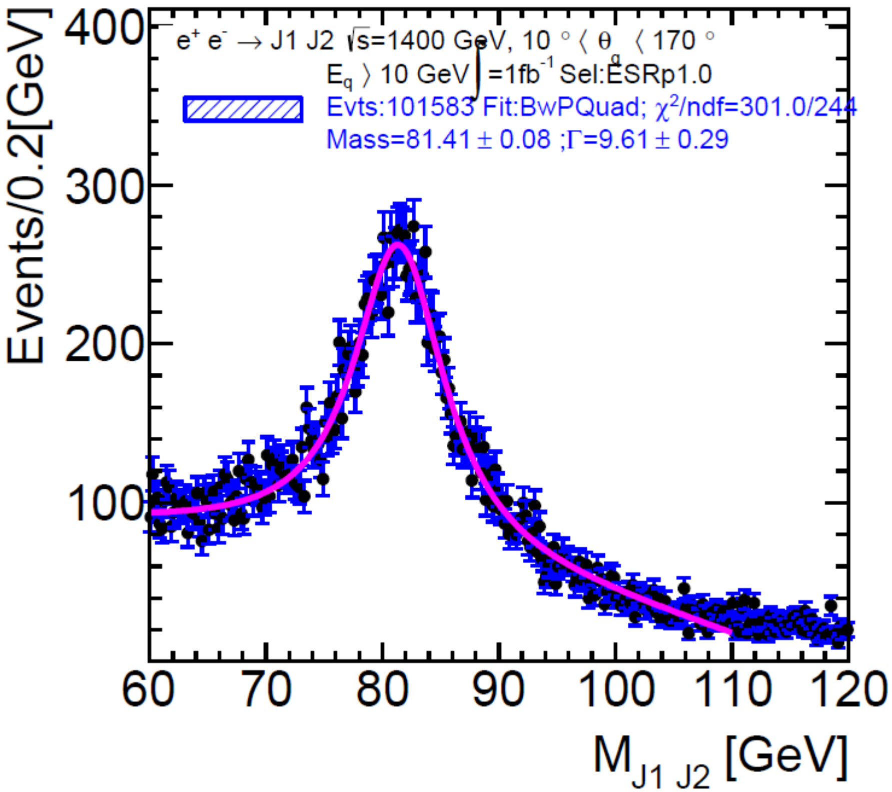

Zoom in Z, W region; Z not visible

MZ=81.4 ± 0.08 GeV; ΓW=9.6 GeV; the resolution doesn't allow an accurate determination of the di-jet energy scale.